

Spontaneous formation of $\text{Cu}_2\text{O-g-C}_3\text{N}_4$ core-shell nanowires for photocurrent and humidity responses

Lixia Wang, Fei Zhao, Qing Han, Chuangang Hu, Lingxiao Lv, Nan Chen, and Liangti Qu*

Beijing Key Laboratory of Photoelectronic/Electrophotonic Conversion Materials;

Key Laboratory of Cluster Science, Ministry of Education of China;

School of Chemistry, Beijing Institute of Technology, Beijing 100081, China

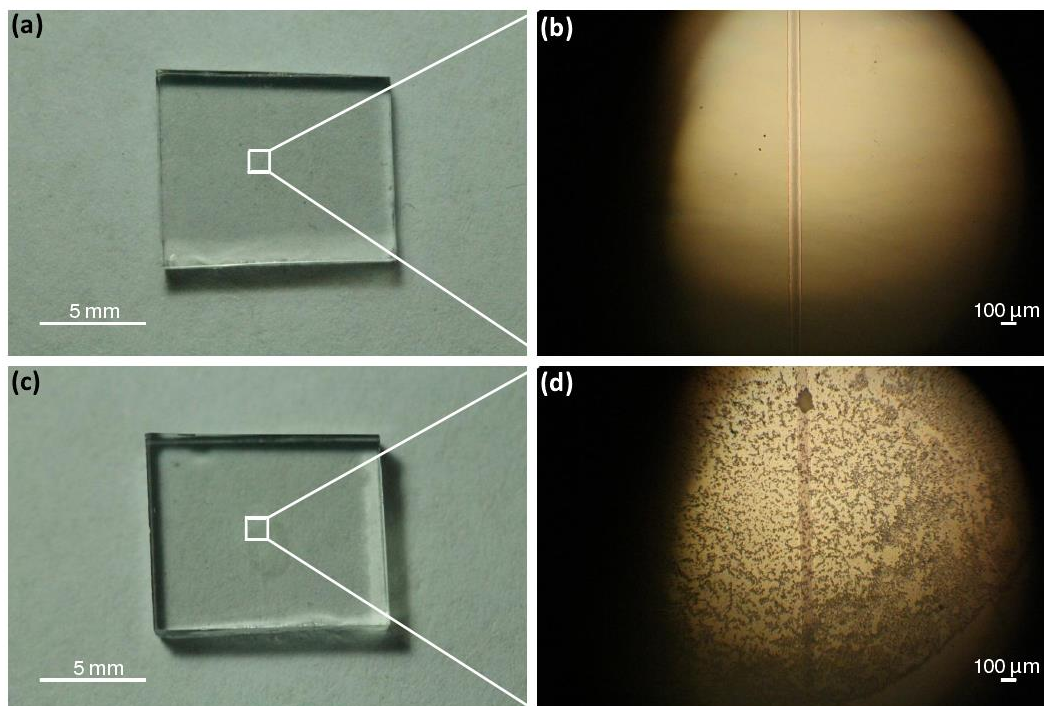


Fig. S1 (a) The photograph of the prepared FTO electrode. (b) The magnified optical microscope photograph of the white box area in (a). (c) The photograph of $\text{Cu}_2\text{O-g-C}_3\text{N}_4$ core-shell nanowires-coated FTO sensor. (d) The magnified optical microscope photograph of the white box area in (c). Scale bars: (a, c), 5 mm; (b, d), 100 μm .

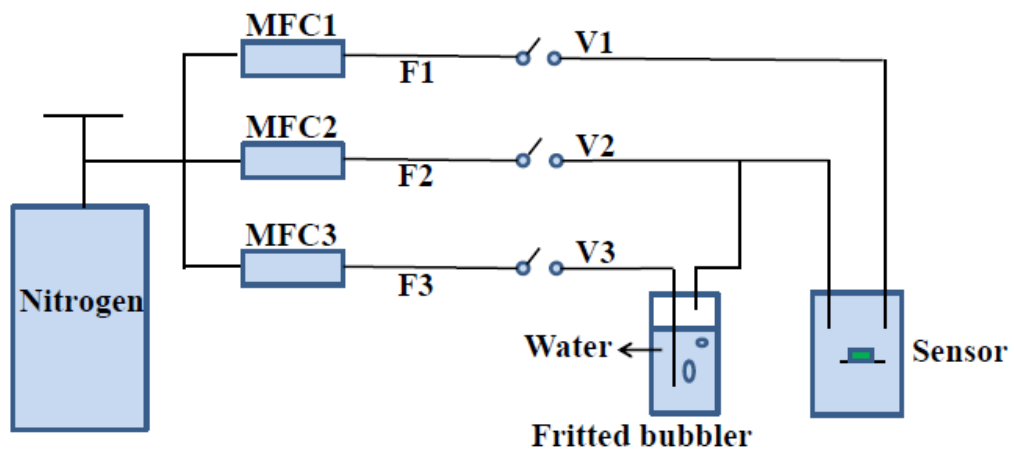


Fig. S2 Test arrangement. Flow F3 generates a constant saturated humidity, Flow F2 dilutes it and Flow F1 provides dry reference.

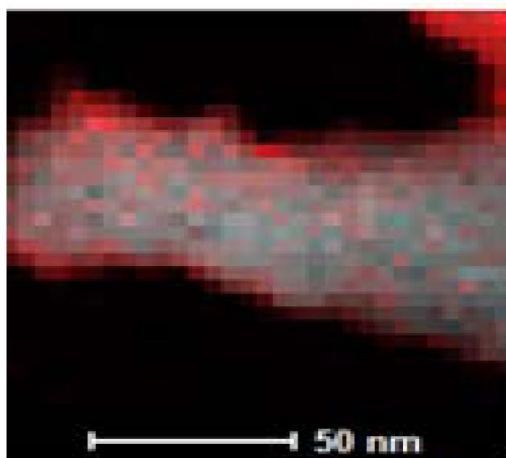


Fig. S3 The overlay chart of the elemental mapping images of C and Cu elements of the prepared $\text{Cu}_2\text{O-g-C}_3\text{N}_4$ core-shell nanowires. Scale bar: 50 nm.

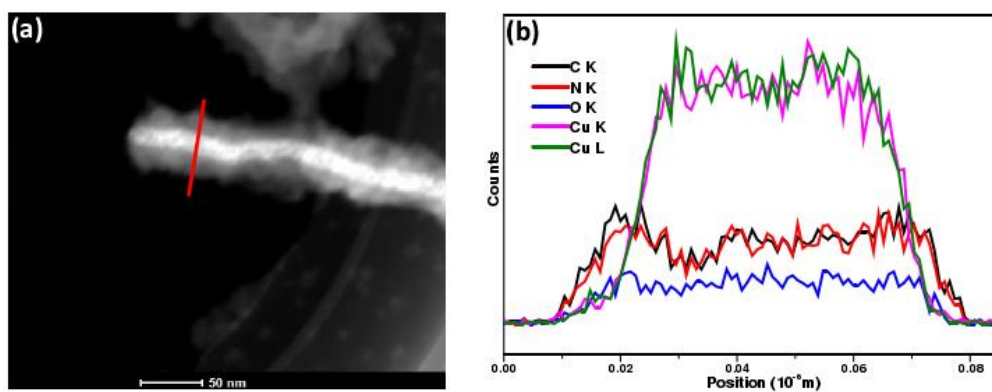


Fig. S4 (a) HAADF image of the prepared $\text{Cu}_2\text{O-g-C}_3\text{N}_4$ core-shell nanowires. The red line in (a) is the position of the elemental line-scanning. (b) Elemental line-scanning image of C, N, O and Cu elements, respectively. Scale bar: (a), 50 nm.

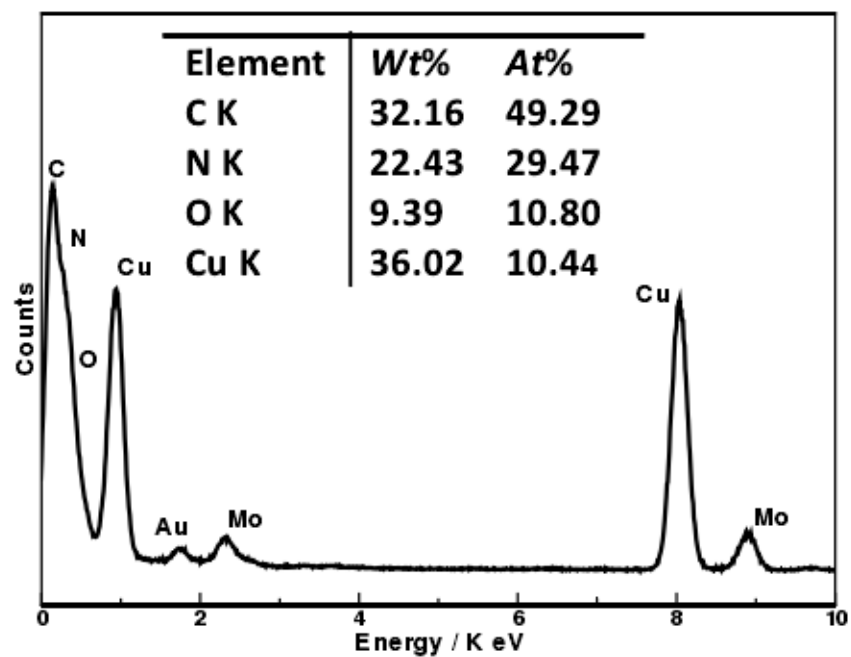


Fig. S5 EDS spectrum and the corresponding contents of C, N, O and Cu of $\text{Cu}_2\text{O-g-C}_3\text{N}_4$ core-shell nanowires. The peaks of Mo and Au are attributed to the Mo micro-grid substrate used.

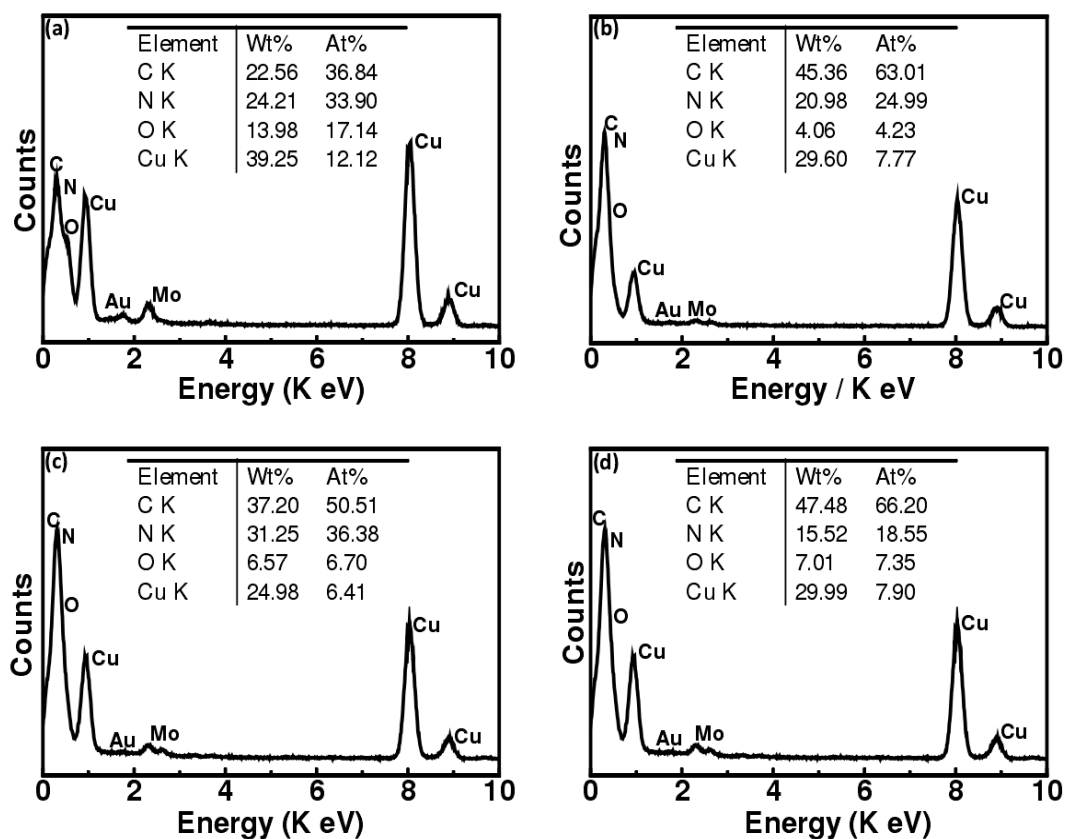


Fig. S6 EDS spectra and the corresponding contents of C, N, O and Cu of Cu₂O-g-C₃N₄ core-shell nanowires with different growth conditions. (a) 48 h and (b) 144 h with 1 mg mL⁻¹ of O-functional g-C₃N₄ solution, (c) 96 h with 0.1 mg mL⁻¹ of O-functional g-C₃N₄ solution, (d) 96 h with 0.3 mg mL⁻¹ of O-functional g-C₃N₄ solution. The peaks of Mo and Au are attributed to the Mo micro-grid substrate used.

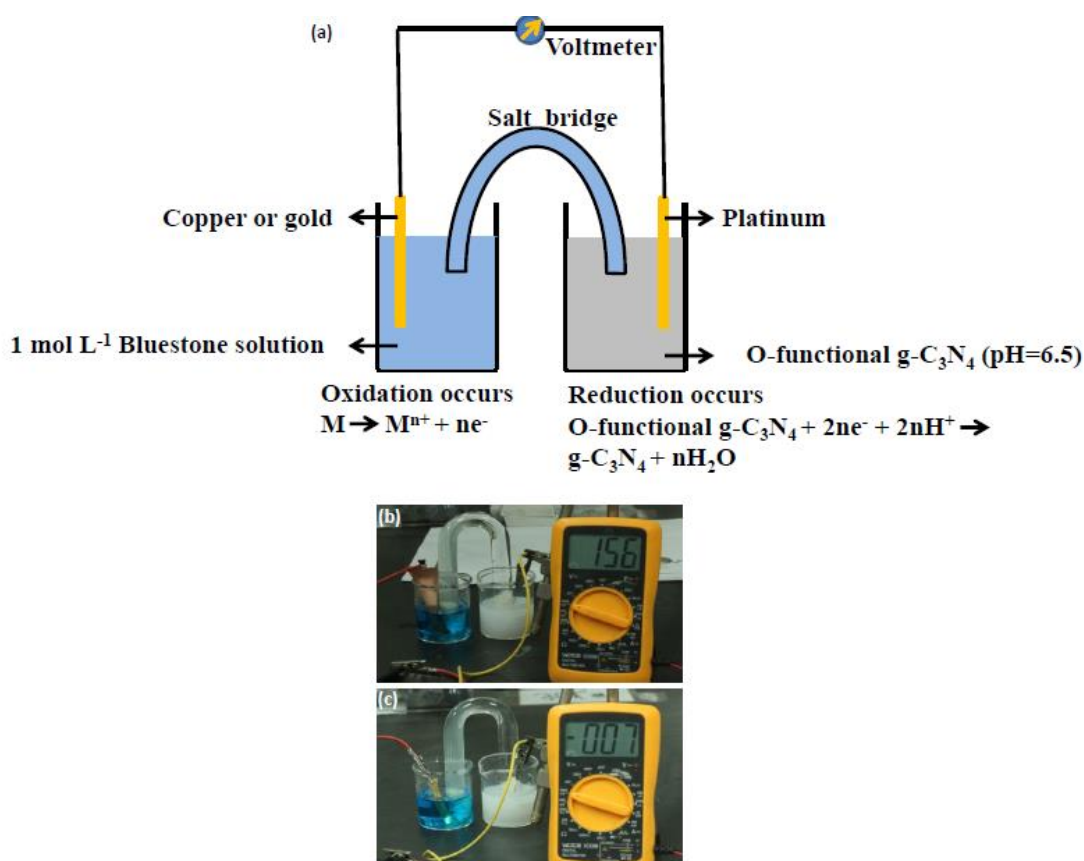


Fig. S7 (a) Schematic description of the designed galvanic cell. Cu and Au foils were used as the anode and inert platinum was used as the cathode. A salt bridge was used to allow the flow of current. In the anode compartment, the electrolyte was 1 mol L⁻¹ bluestone solution. In the cathode compartment, the electrolyte was O-functional g-C₃N₄ solution with pH=6.5. Before measurements, the electrolytes were saturated with nitrogen. Oxidation occurred at the anode and provided electrons ($M \rightarrow M^{n+} + ne^{-}$). O-functional g-C₃N₄ would accept the electrons and be reduced at the cathode ($n \text{ O-functional } g\text{-C}_3\text{N}_4 + 2ne^{-} + 2nH^{+} \rightarrow g\text{-C}_3\text{N}_4 + nH_2O$). (b) The cell (-) Cu|Cu²⁺|| O-functional g-C₃N₄| g-C₃N₄ (+) could generate a cell voltage of 156 mV. So, according to the relationship between the thermodynamic function and the cell voltage ($\Delta G = -nFE$), the redox reaction between O-functional g-C₃N₄ and copper was spontaneous. (c) The cell (-) Au|Au³⁺|| O-functional g-C₃N₄| g-C₃N₄ (+) only generated a very small voltage (~ -7 mV) that might be caused by the concentration potential and liquid junction potential. So, gold could not be used to reduce O-functional g-C₃N₄.

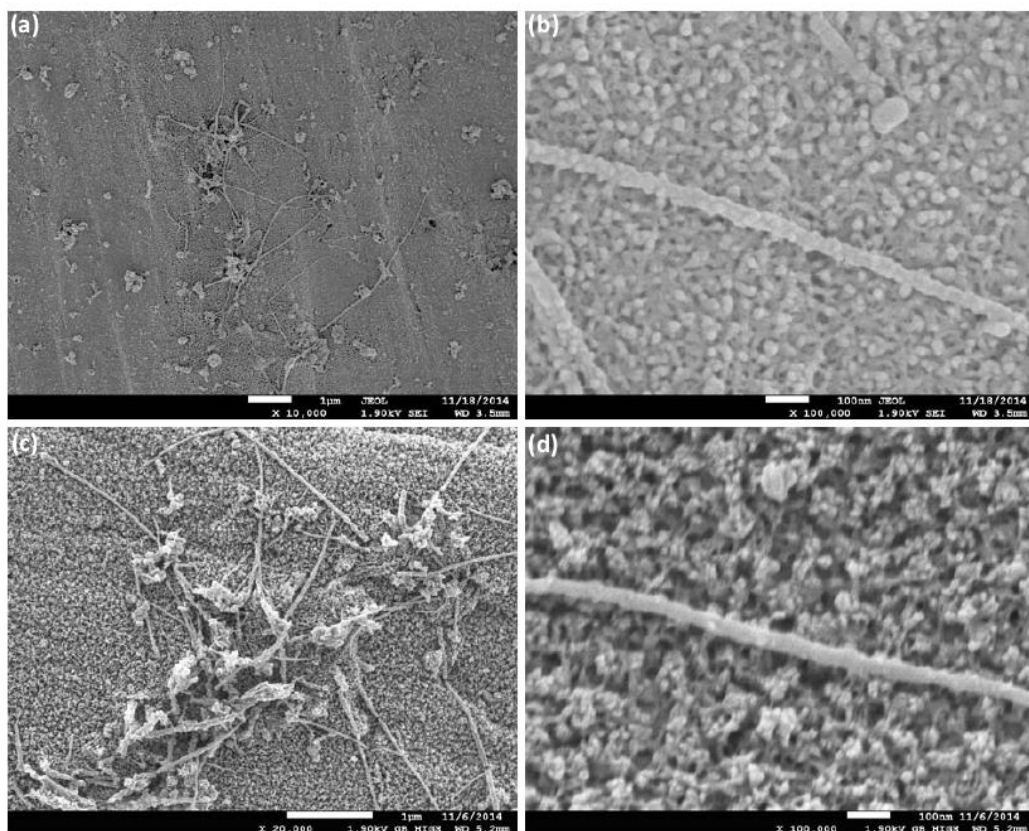


Fig. S8 The SEM images of $\text{Cu}_2\text{O-g-C}_3\text{N}_4$ core-shell nanowires kept still for 96 h with different concentrations of O-functional g- C_3N_4 solution (a, b) 0.1 mg mL^{-1} , (c, d) 0.3 mg mL^{-1} . Scale bars: (a, c), $1 \mu\text{m}$; (b, d), 100 nm .

In addition, When the concentration is 0.1 mg mL^{-1} , $\text{Cu}_2\text{O-g-C}_3\text{N}_4$ core-shell nanowires has formed, but the amount was less. With increasing the concentration to 0.3 mg mL^{-1} , there is almost no change of the structure of $\text{Cu}_2\text{O-g-C}_3\text{N}_4$ core-shell nanowires but more amounts appeared.

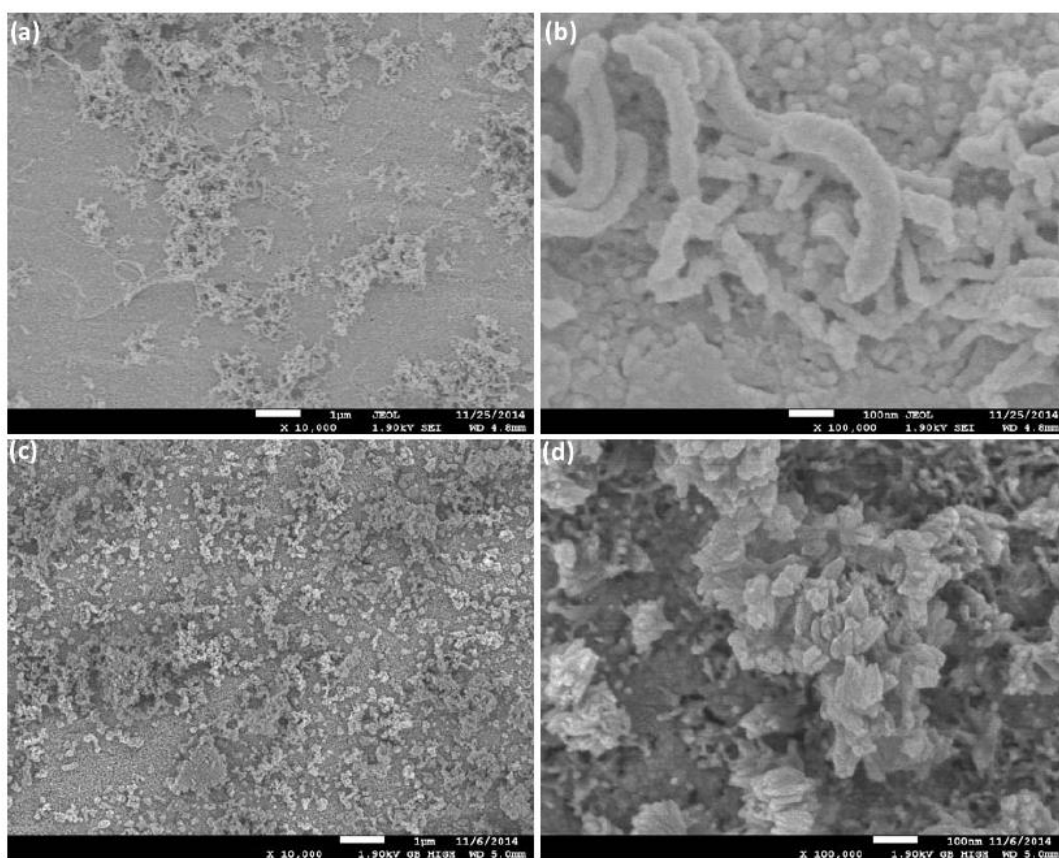


Fig. S9 The SEM images of Cu_2O - $\text{g-C}_3\text{N}_4$ core-shell nanowires kept still for 96 h in dark (a, b) and under illumination (c, d). Scale bars: (a, c), 1 μm ; (b, d), 100 nm.

Given the excellent photocatalytic activity of $\text{g-C}_3\text{N}_4$ under visible light, the illumination contrast experiments were conducted at identical experimental conditions to explain further the reaction process. Compared with the long and thick nanowires prepared under normal indoor lighting, short and thin nanowires formed on the surface of Cu under totally dark condition, indicating the main drive force to contribute the reaction should be oxidation-reduction between the O-functional $\text{g-C}_3\text{N}_4$ and Cu, illumination only accelerating it. While the sample was irradiated under a 300 W Xe lamp, flower-like nanoclusters formed on the surface of Cu foil probably because the accelerating reaction between the O-functional $\text{g-C}_3\text{N}_4$ and Cu under illumination caused the disorder stack of $\text{g-C}_3\text{N}_4$.

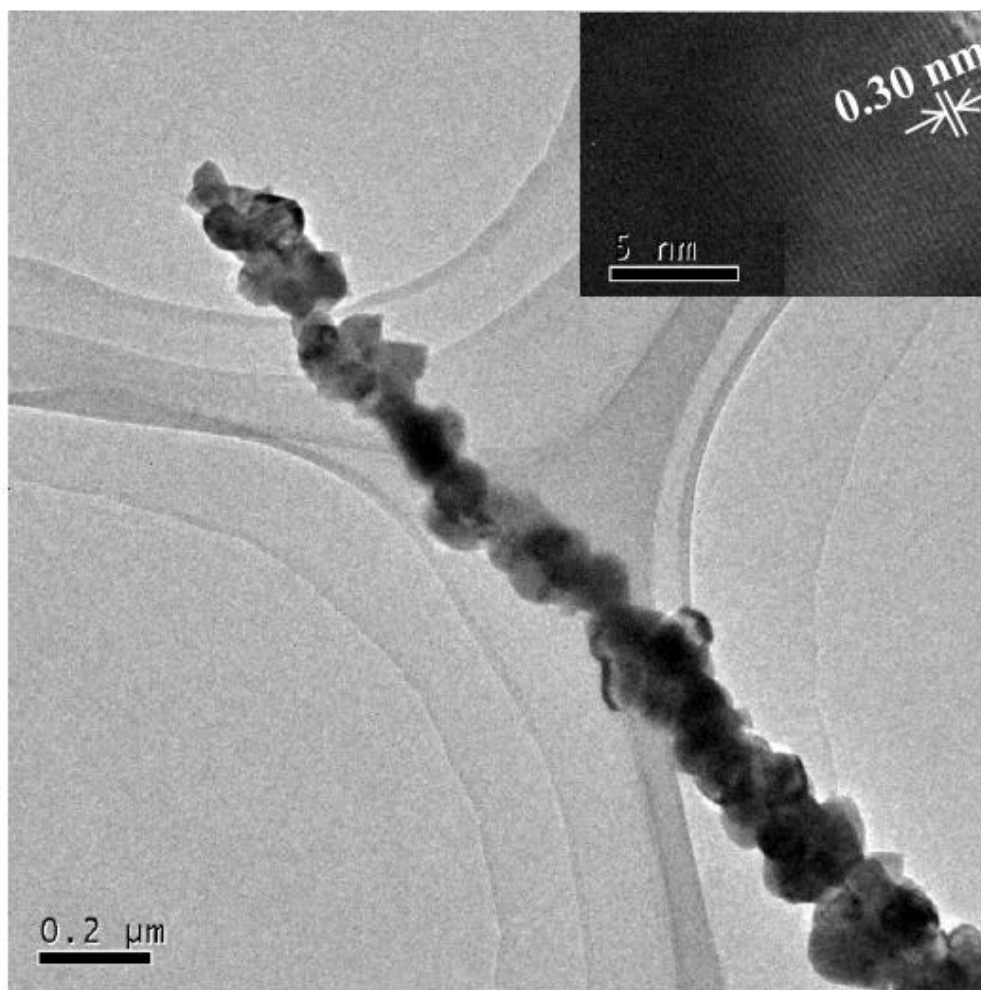


Fig. S10 The TEM of the contrast Cu₂O nanowires. The inset is the magnified image of of the Cu₂O nanowires.

In accordance with the solution-grown condition at room temperature for Cu₂O-g-C₃N₄ core-shell nanowires, a similar process was choosed for the preparation of the contrast Cu₂O nanowires.¹ The HRTEM image of the Cu₂O nanowires show interplanar spacing of 0.30 nm, consistent with the (110) lattice planes of cubic-phase Cu₂O, which is well matched with that in the XRD pattern (Figure 2g (ii)). Scale bars: 0.2 μm; The inset, 5 nm.

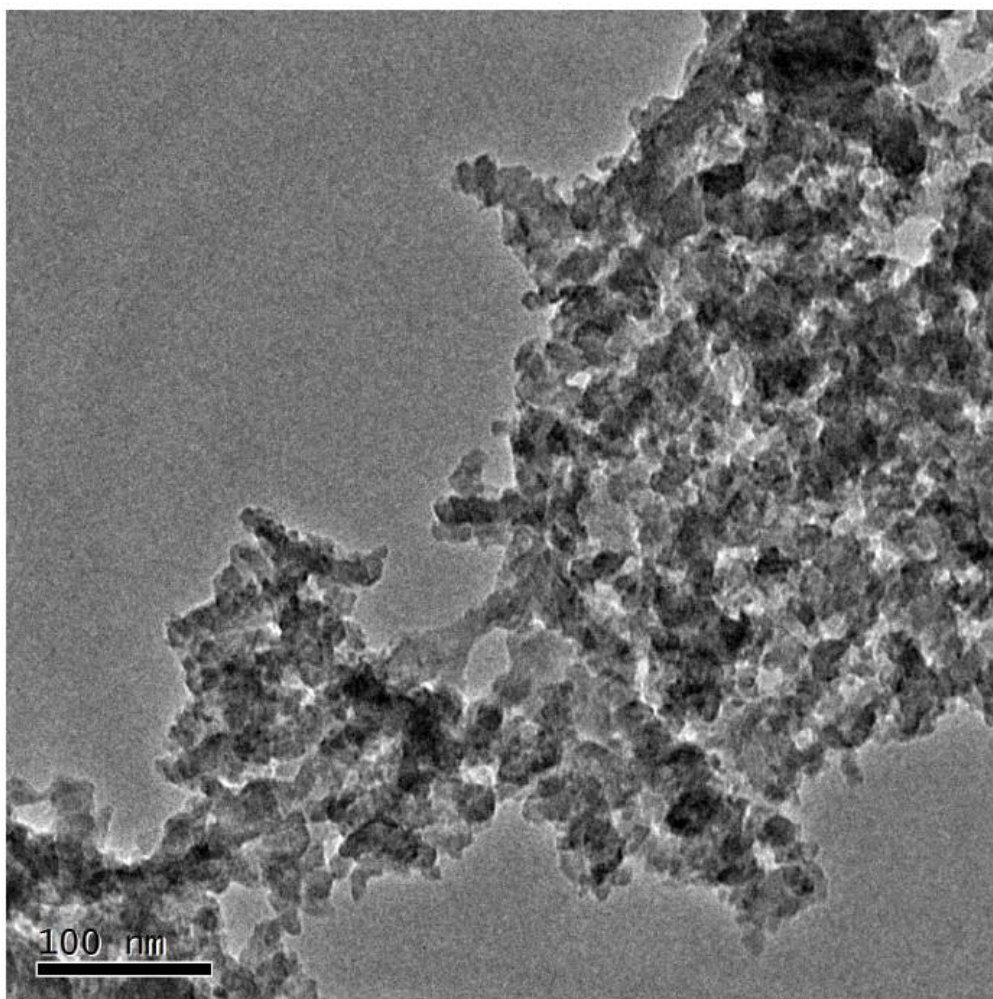


Fig. S11 The TEM image of the g-C₃N₄. Scale bar: 100 nm.

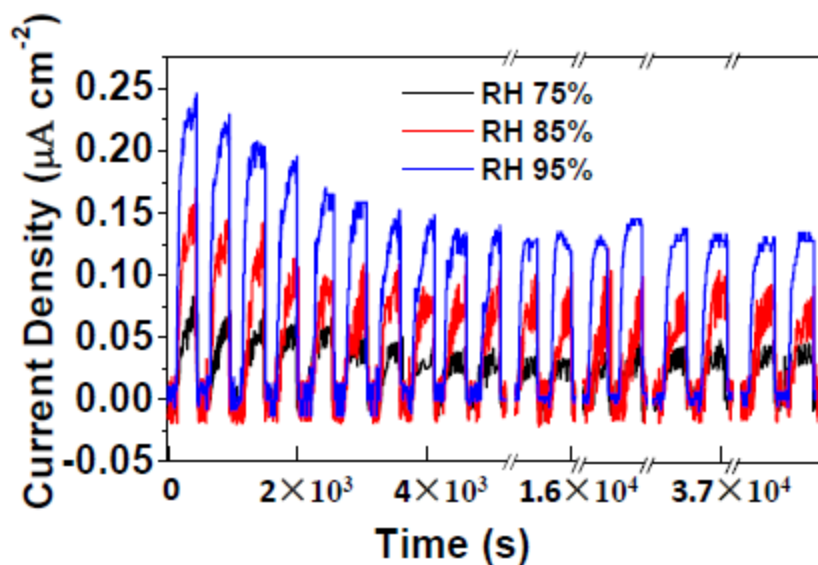


Fig. S12 Current response of $\text{Cu}_2\text{O-g-C}_3\text{N}_4$ core-shell nanowires-coated FTO sensors to dynamic switches between dry air (0%) and different (75%–95%) RH at 30 °C for 100 cycles. The first 10 cycles in the figure were the first 10 cycles of the 100 cycles, the eleventh (11th) and twelfth (12th) cycles correspond to the 29th and 30th cycles of the 100 cycles, 13th and 14th cycles to the 49th and 50th cycles, 15th (69th), 16th (70th), 17th (99th) and 18th (100th).

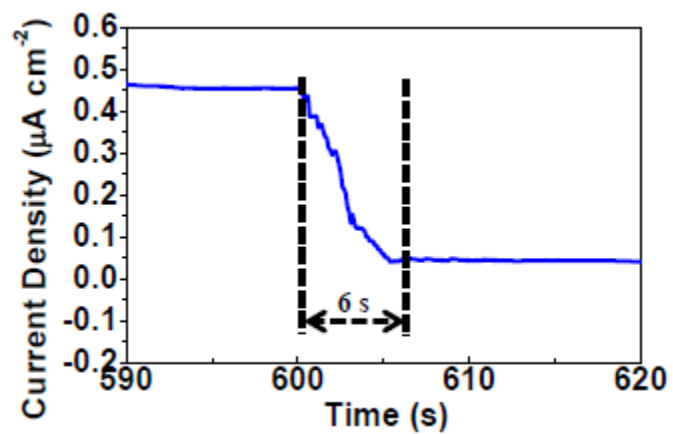


Fig. S13 The enlarged image of the recovery process in the Fig. 6e.

References

- [s1] A. Kargar, S. S. Partokia, M. T. Niu, P. Allameh, M. Yang, S. May, J. S. Cheung, K. Sun, K. Xu and D. L. Wang, *Nanotechnology*, 2014, **25**, 1.